Journal of Photochemistry & Photobiology, A: Chemistry 459 (2025) 116108

Contents lists available at ScienceDirect

Journal of Photochemistry & Photobiology, A: Chemistry

journal homepage: www.elsevier.com/locate/jphotochem

Preparation of cysteine-functionalized graphene quantum dots – Zinc phthalocyanines supramolecular hybrid system and their sono-photochemical studies

Gökçe Gökçil [a], Göknur Yaşa Atmaca [a,*], Pınar Şen [b,c], Fikrettin Şahin [b], Ali Erdoğmuş [a,d]

[a] Department of Chemistry, Yildiz Technical University, Esenler, Istanbul 34210, Turkey
[b] Department of Genetics and Bioengineering, Yeditepe University, Ataşehir, Istanbul 34755, Turkey
[c] Department of Chemical Engineering, Üsküdar University, 34662 Üsküdar, Istanbul, Turkey
[d] Health Biotechnology Joint Research and Application Center of Excellence, 34220 Istanbul, Turkey

ARTICLE INFO

Keywords:
Phthalocyanines
Photodynamic therapy (PDT)
Photosensitizer
Sono-photodynamic therapy
Graphene quantum dots
Singlet oxygen

ABSTRACT

Current PDT agents often suffer from low singlet oxygen quantum yields, photobleaching, and poor biocompatibility. To address these issues, we propose novel PDT agents that combine the synthesized phthalocyanines with cysteine-functionalized graphene quantum dots (cys-GQDs) for the first time. This combination aims to enhance singlet oxygen production and improve solubility in biological media. In this way, new zinc phthalocyanines with halogen substituents were synthesized for potential use in photodynamic therapy (PDT). Specifically, 2-Bromo-4-methylphenol zinc (II) phthalocyanine (**2a**) and 2-chloro-4-methylphenol zinc(II) phthalocyanine (**2b**) and their graphene quantum dots derivatives were synthesized and characterized. The photochemical, sonochemical, and sono-photochemical properties of these compounds were analyzed, focusing on their efficiency in singlet oxygen production. Our studies of the **2a**@cys-GQDs and **2b**@cys-GQDs conjugates demonstrated higher singlet oxygen yields, suggesting their enhanced potential for clinical applications.

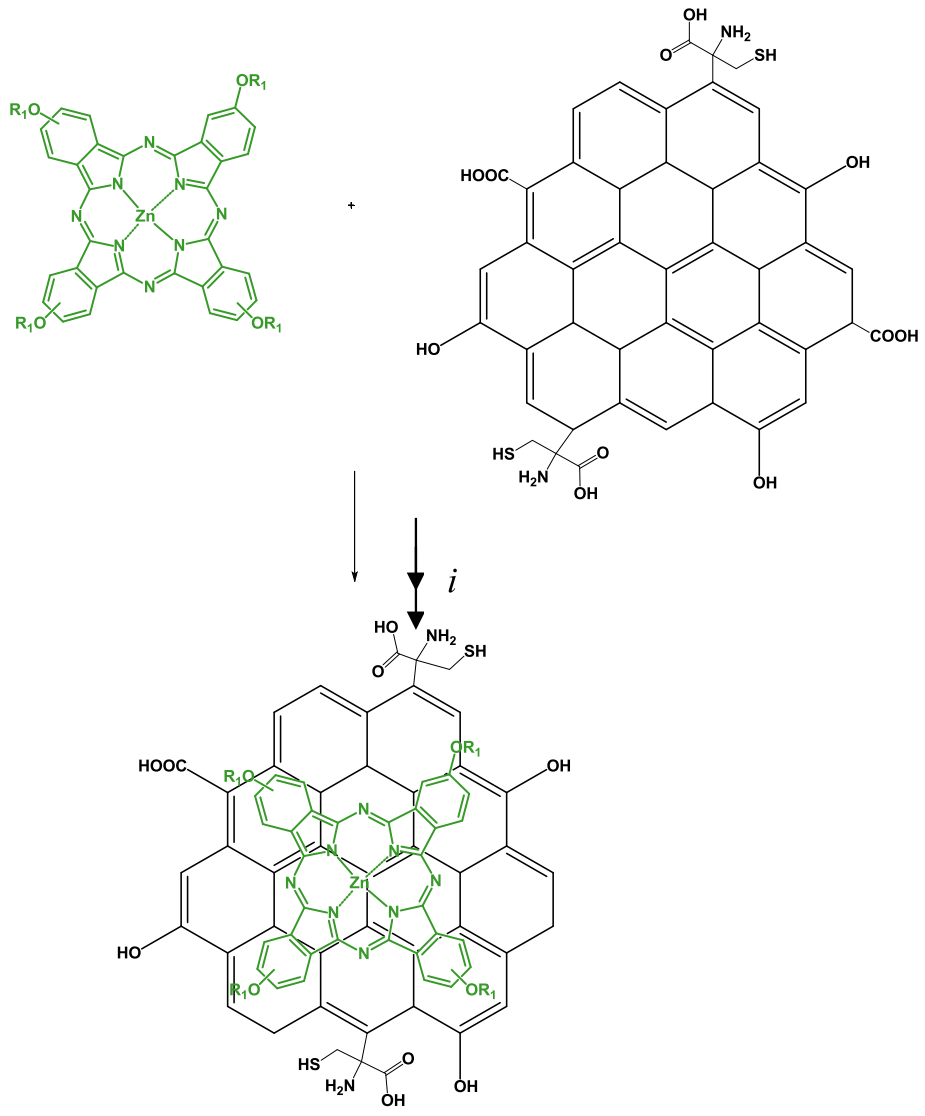
1. Introduction

Cancer is a disease defined by the growth of abnormal cells that grow out of control and have the capacity to invade and destroy healthy body tissues. There are many traditional therapies such as chemotherapy and radiotherapy, but these can have negative affect on people [1,2]. Because of that, new treatment methods are being developed, including photodynamic therapy (PDT), which can be applied without surgery. PDT offers various advantages, including selective accumulation in tumor cells, low toxicity, and cost-effectiveness. Additionally, it is reproducible, facilitates rapid recovery, and enhances the patient's quality of life [2–4]. In this method, singlet oxygen is transferred to the cancer cell to cause apoptosis or necrosis when the tumor area is irradiated with light of the appropriate wavelength [5–8]. Sonodynamic therapy (SDT) is another method inspired by PDT applied for therapeutic efficacy [9–12]. SDT is activated by ultrasound instead of light and that is the most important difference between them [12,13]. In recent years, a new method called sono-photodynamic therapy (SPDT) has been developed with the synergistic effect of PDT and SDT [13]. Compared to either monotherapy, this combined therapy has demonstrated more impressive anti-cancer benefits [14,15]. This therapy is based on the administration of a tiny quantity of a sensitizer. This sensitizer can be concurrently activated by ultrasound and light to create mechanical, photochemical, and sonochemical activities. The sensitizers should not be very toxic, have a high sono-photo sensitivity, and have a good clearance rate from healthy tissues [16,17]. Phthalocyanines are second-generation photosensitizers, preferred for their exceptional photophysical and photochemical qualities. These include their lack of dark toxicity, deeper tissue penetration, high singlet oxygen generation yield, strong absorbance at long wavelengths (650–1050 nm), and chemical stability [18]. As the central metal atoms and groups substituted to the ring are changed, the therapeutic effects required for use in PDT can be improved [19–21].

Nanomedicines have experienced major developments and increasing interest since the late 1990s. Among the studied nanoparticles, graphene quantum dots (GQDs) has found a wide field of application in recent years due to its unique optical, electrical and optoelectrical properties. The non-toxic, biologically inert properties of

* Corresponding author.
E-mail address: gyasa@yildiz.edu.tr (G.Y. Atmaca).

https://doi.org/10.1016/j.jphotochem.2024.116108
Received 6 August 2024; Received in revised form 4 October 2024; Accepted 18 October 2024
Available online 24 October 2024
1010-6030/© 2024 Elsevier B.V. All rights are reserved, including those for text and data mining, AI training, and similar technologies.



Scheme 1. Synthetic route of two new phthalonitriles (**1a**,**1b**), (i) DMF, K_2CO_3, 24 h; and their zinc phthalocyanines derivatives (**2a**, **2b**), (ii) anhydrous $Zn(Ac)_2$, penthanol, DBU, argon atm, 15 h.

GQDs and their chemical and physical stability have attracted worldwide academic interest [22]. In addition to these properties, GQDs exhibited many important characteristics such as good solubility, surface grafting and biocompatibility, which prompted many potential applications of GQDs in fluorescent agents [23], bioimagings [24], sensors [25], drug carriers [26] and as photosensitizers in photodynamic therapy [27]. Recent researches showed that drug carrier properties can be enhanced by surface modifications or modified by functional groups [28]. The presence of delocalized π electrons of GQDs facilitates the interaction of phthalocyanines which are rich in delocalized π electrons through non-covalent π–π stacking. It is expected that combining the two PDT agents (phthalocyanines and GQDs) will result in improved PDT action through a synergistic effect since GQDs are well known PDT agents with high singlet oxygen quantum yields [29].

The aim in this study was to synthesize new phthalocyanines with improved singlet oxygen efficiency thanks to their graphene quantum dots derivatives that can be used in photodynamic therapy and sono-photodynamic therapy. For this purpose, 2-Bromo-4-methylphenol and 2-Chloro-4-methylphenol materials and metallized phthalocyanines with zinc central atoms were synthesized and characterized. Then the cysteine-functionalized GQDs (cys-GQDs) were obtained and the synthesized Pcs were conjugated to cys-GQDs. Finally, the sono-photochemical properties of all synthesized phthalocyanines and the cys-GQDs were investigated and compared. This will be the first example involving the interaction of phthalocyanines with cys-GQDs for sono-photochemical studies.

2. Experimental

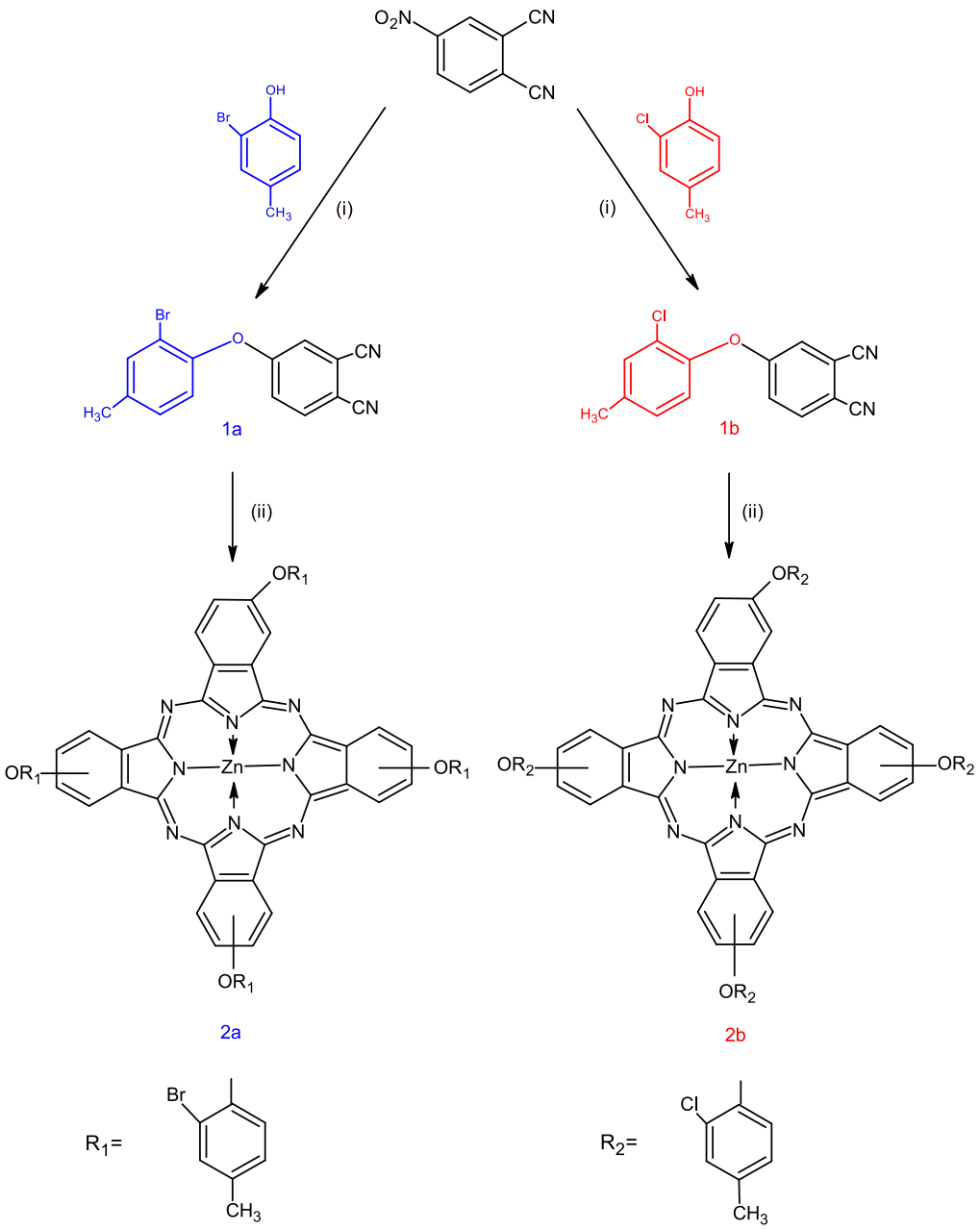
2.1. Materials and equipment

All materials and equipment utilized in this study are listed in the supplementary material.

2.2. Synthesis

2.2.1. Synthesis of 2-Bromo-4-methylphenol phthalonitrile (*1a*)

4-Nitrophthalonitrile (1 g, 5.3 mmol) was dissolved with DMF under argon gas and 2-Bromo-4-methylphenol (1 g, 5.3 mmol) was added. After stirring at room temperature for 30 min, anhydrous potassium carbonate (2.21 g, 16.04 mmol) was added. The reaction was stirred under argon gas at room temperature for 24 h. The resulting mixture was precipitated in 200 ml of ice water and filtered. The filtrate was washed with plenty of water to remove the potassium carbonates and finally



Scheme 2. An illustration of route for the π–π stacked conjugate: (i) sonicate, 4 h, stir room temperature, 4 d.

washed in methanol. The dried product was crystallized from the ethanol-methanol mixture and dried in vacuum. A pure white product was obtained. Yield: 28 %. IR spectrum (cm^{-1}): 2232 (C≡N), 1249 (C—O—C), 3081 (C—H), 1589 (C=C), 794 (C—Br). ^{1}H NMR (500 MHz, δppm): 7.75 (s, 1H, Ar—H), 7.73 (s, 1H, Ar—H), 7.54 (d, 2H, Ar—H), 7.37 (d, 2H, Ar—H), 1.59 (s, 3H, —CH_3). MS (MALDI-MS) *m/z*: Calculated: 313.148 for $C_{15}H_9BrN_2O$; Found: 310.787 $[M-2H]^+$.

2.2.2. *Synthesis of 2-Chloro-4-methylphenol phthalonitrile (**1b**)*

4-Nitrophthalonitrile (1 g, 7.01 mmol) was dissolved with DMF under argon gas and 2-Chloro-4-methylphenol (1 g, 7.01 mmol) was added. After stirring at room temperature for 30 min, anhydrous potassium carbonate (2.90 g, 21.04 mmol) was added. The reaction was stirred under argon gas at room temperature for 24 h. The resulting mixture was precipitated in 200 ml of ice water and filtered. The filtrate was washed with plenty of water to remove the potassium carbonates and finally washed in methanol. The dried product was crystallized from the ethanol-methanol mixture and dried in vacuum. A pure white product was obtained. Yield: 32 %. IR spectrum (cm^{-1}): 2232 (C≡N), 1250 (C—O—C), 3000–3100 (C—H), 1590 (C=C), 799 (C-Cl). ^{1}H NMR (500 MHz, δppm): 7.75 (s, 1H, Ar—H), 7.73 (s, 1H, Ar—H), 7.57 (d, 2H, Ar—H), 7.08–7.06 (d, 2H, Ar—H), 1.58 (s, 3H, —CH_3). MS (MALDI-MS) *m/z*: Calculated: 268.697 for $C_{15}H_9ClN_2O$; Found: 270.883 $[M+2H]^+$.

2.2.3. *Synthesis of 2-Bromo-4-methylphenol zinc (II) phthalocyanine (**2a**)*

Compound **1a** (0.1 g, 0.32 mmol), anhydrous zinc acetate (0.05 g, 0.027 mmol), 4 drop DBU and 4 ml dry pentanol in a reaction tube under argon atmosphere at 120 °C for 24 h mixed. The green mixture, which was then cooled to room temperature, was precipitated dropwise into 200 ml of n-hexane. The precipitated core product was purified by washing with hot hexane, ethanol and methanol. Finally, TLC was measured in the raw product. Chloroform was used as the running solvent. Yield: 51 %. IR spectrum (cm^{-1}): 1205 (C—O—C), 3281 (C—H), 1597 (C=C), 744 (C—Br).^{1}H NMR (500 MHz, δppm): 7.86–7.49 (m,

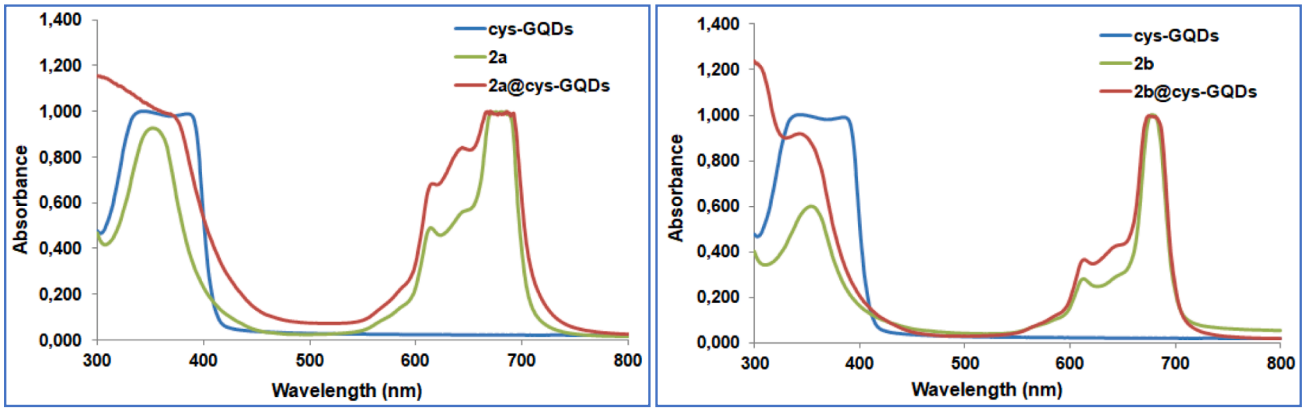


Fig. 1. Normalized electronic absorption spectra of (a) cys-GQDs, **2a**, **2a**@cys-GQDs, (b) cys-GQDs, **2b**, **2b**@cys-GQDs.

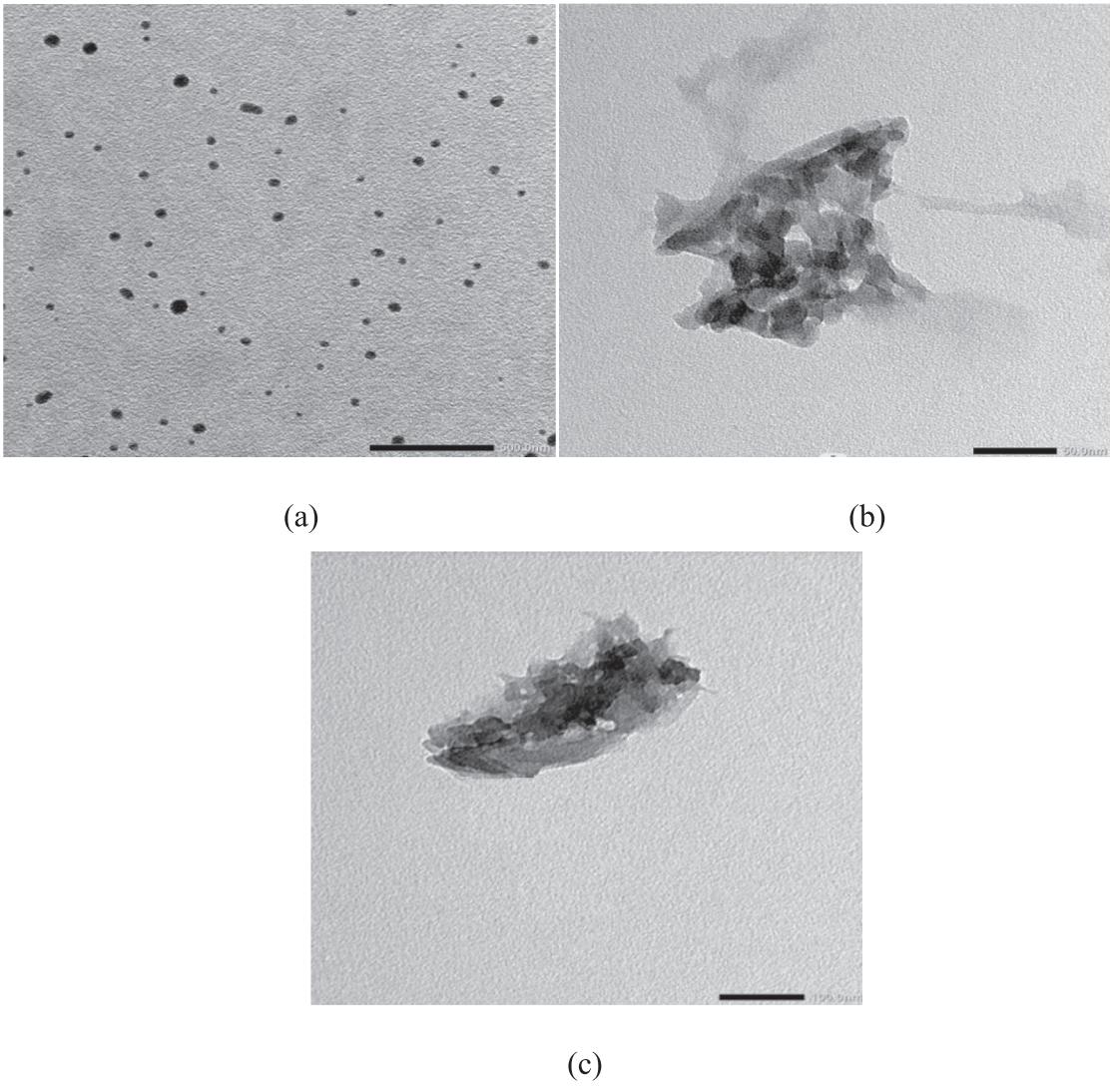


Fig. 2. Transmission electron micrographs for (a) cys-GQDs, (b) **2a**@cys-GQDs, (c) **2b**@cys-GQDs.

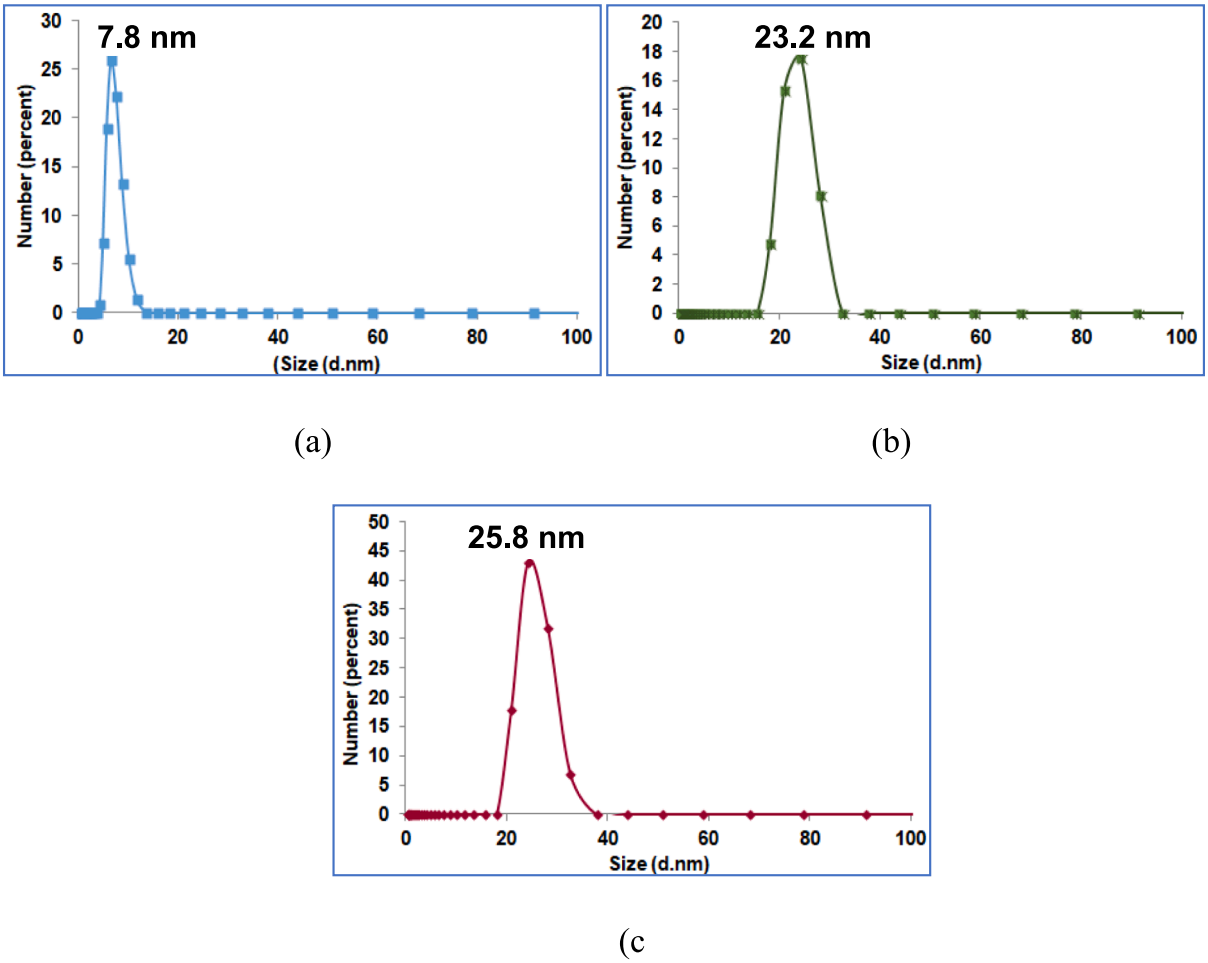


Fig. 3. Dynamic light scattering (DLS) showing average particle sizes of (a) cys-GQDs, (b) **2a**@cys-GQDs, (b) **2b**@cys-GQDs.

24H, Ar—H), 1.59 (s, 12H, —CH_3). MS (MALDI-MS) *m/z*: Calculated: 1318.00 for $C_{60}H_{36}Br_4N_8O_4Zn$; Found: 1318.45 $[M]^+$.

*2.2.4. Synthesis of 2-Chloro-4-methylphenol zinc (II) phthalocyanine (**2b**)*

Compound **1b** (0.1 g, 0.37 mmol), anhydrous zinc acetate (0.05 g, 0.027 mmol), 4 drop DBU and 4 ml dry pentanol in a reaction tube under argon atmosphere at 120 °C for 24 h mixed. The green mixture, which was then cooled to room temperature, was precipitated dropwise into 200 ml of n-hexane. The precipitated core product was purified by washing with hot hexane, ethanol and methanol. Finally, TLC was measured in the raw product. Chloroform was used as the running solvent. Yield: 55 %. IR spectrum (cm^{-1}): 1205 (C—O—C), 3252 (C—H), 1597 (C=C), 744 (C-Cl).^{1}H NMR (500 MHz, δppm): 7.83–7.35 (m, 24H, Ar—H), 1.60 (s, 12H, —CH_3). MS (MALDI-MS) *m/z*: Calculated: 1140.200 for $C_{60}H_{36}Cl_4N_8O_4Zn$; Found: 1140.707 $[M]^+$.

2.2.5. Synthesis of cys-GQDs

cys-GQDswere synthesized using with citric acid as a carbon source and Cystein amino acid as a sulfur and nitrogen source using the literature method with some modification [30]. Briefly, 1 g citric acid and 0.5 g cysteine were dissolved in 3 mL of DI water. The obtained solution was hydrothermally treated at 220 °C for 12 h under N_2 gas. Afer that, the reddish-brown mixture was filtered. This suspension was purifed with a dialysis membrane (12–14 kD, Fisher Scientifc) against DI water for 24 h and then precipitated in excess amount of acetone by using a centrifuge at 6000 rpm for 10 min. Finally, cys-GQDs were dried in an oven at 50 °C and stored in a closed container for further applications.

2.2.6. Pc-GQDs conjugate synthesis

The ZnPcs (**2a** and **2b**) conjugation of cys-GQDs based on π–π stacking was performed by way of a slight modification to the previously reported literature [31]. Briefly, the solution of 12.5 mg of cys-GQDs (in 1 mL H_2O) and the solutions of 25 mg of ZnPc (**2a**) (0.5 ml in DMF) and 25 mg ZnPc (**2b**) (0,5 ml in DMF) were sonicated for 1 h seperately. Then, cys-GQDs solution was added to the solutions of ZnPcs and the mixtures was sonicated for 4 h then stirred at room temperature for 4 d. The mixture was precipitated with ethanol and washed with water and ethanol. The product was dried in a laboratory oven at 60 °C to obtain Pc@ cys-GQDs. The obtained nanocompozites are represented as **2a**@ cys-GQDs and **2b**@cys-GQDs.

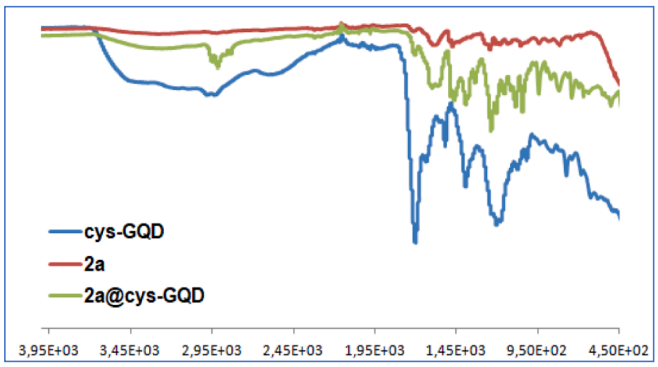
2.3. Photophysical and photochemical studies

The fluorescence quantum yield, a photophysical property, and the singlet oxygen quantum yield and photodegradation quantum yield, as photochemical properties, were assessed using the methods detailed in the supplementary material.

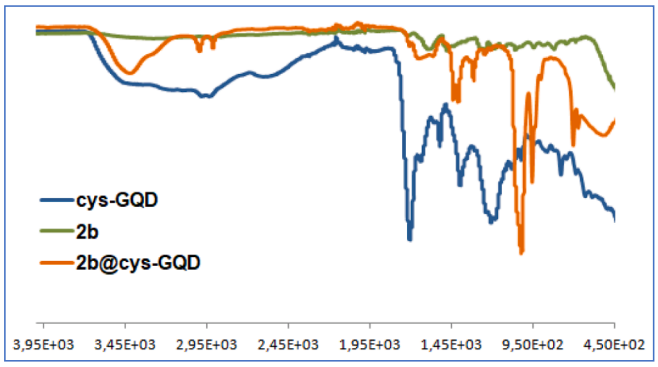
3. Results and discussion

3.1. Syntheses and characterization

New zinc phthalocyanines designed for high singlet oxygen efficiency were synthesized, as shown in Scheme 1. These compounds are intended for use in the PDT method, which serves as an alternative approach to cancer treatment. These new complexes were prepared by



(a)



(b)

Fig. 4. The comparative FT-IR spectra of (a) cys-GQDs,**2a**, **2a**@cys-GQDs, (b) cys-GQDs, **2b**, **2b**@cys-GQDs.

the template cyclotetramerization of 2-Bromo-4-methylphenol phthalonitrile (**1a**) ve 2-Chloro-4-methylphenol phthalonitrile (**1b**) and anhydrous $Zn(OAc)_2$ in the presence of dry pentanol and DBU at reflux temperature under argon atmosphere. Although phthalocyanines are generally not well soluble in organic solvents, the synthesized PCs were well soluble in DMSO. The complexes were characterized by using the UV–Vis, FT-IR, ^{1}H NMR and mass spectroscopy techniques. Afterwards, photophysical and photochemical properties of the compounds were investigated to estimating their potential for anti-cancer therapy.

As the second stage, The prepared phthalocyanines was conjugated to cys-GQDs via π–π stacking. The obtained nanocomposite was characterized by using analytical techniques such as XRD, FT-IR, dynamic light scattering (DLS), UV/vis.The results were confirmed the expected products.

The binding of cys-GQDs to the Pcs through π–π stacking was achieved as represented in Scheme 2.

The UV–Vis spectra of phthalocyanine complexes show characteristic Q and B bands. Q band is in the visible region between 600 and 700 nm and is caused by transitions of $\pi \rightarrow \pi^*$. The B band, were observed in the 300–500 nm region [32,33]. In this study, the Q-band absorptions in the UV–Vis absorption spectra of the phthalocyanines (**2a** and **2b**) were observed at 679 and 680 nm respectively and B bands at 415 nm for both **2a** and **2b** in DMSO.

The UV–Vis absorption spectrum of cys-GQDs shows a strong absorption peak at 344 nm, due to π–π* transition of aromatic structure and 392 nm belonging to n–π* transition of carbonyl groups and C═S bonds of cys-GQDs [34]. The nanoconjugates displayed absorption bands confirming the presence of ZnPcs and the cys-GQDs. There were no noticeable shifts in the Q-bands of the nanoconjugates upon π–π coordination of ZnPcs to the respective GQDs compared to ZnPcs alone. However, there was an increase in absorbance at B band region of the spectra due to the intense absorbance of cys-GQDs (Fig. 1).

The loading amounts of the zinc phthalocyanines onto the cysteine-functionalized graphene quantum dots were determined by spectroscopically through UV–Vis spectrum [35]. Basically, it depends on the absorbance value differences of Pcs before and after loading. The loading of ZnPcs onto cys-GQDs was 76 % for **2b**@cys-GQDs and 62 % for **2a**@cys-GQDs" was added into manuscript.

Transmission electron microscopy (TEM) was used to determine the morphology and shape of the cys-GQDs and its ZnPc conjugates (Fig 2.). A typical TEM image shows spherical graphene quantum dots and monodispersed (Fig. 2a). Upon conjugation of the cys-GQDs to ZnPc complexes (Fig. 2b, c) considerable aggregation was observed. Phyahalocyanines are known to tend to be aggregate upon covalent and/or non-covalent interactions with each other and/or nanoparticles. The formation of stacked conjugates is a result of π–π interaction between ZnPc complexes and adjacent quantum dots rich in π electrons [36].

DLS was used for the determination of particle size forcys-GQDs and its conjugate forms with ZnPc (**2a**) and ZnPc (**2b**). The average size determined by DLS was 7.8 nm for cys-GQDs (Fig. 3a). The observed size distribution is in accordance with typical of GQDs [37]. Upon conjugation of ZnPcs (**2a** and **2b**) onto cys-GQDs, it was acquired an increase in the average particle sizes of cys-GQDs –ZnPcs nanoensembles when compared to cys-GQDs alone. The conjugates **2a**@cys-GQDs and **2b**@cys-GQDs showed a supramolecular diameter sizes 23.2 nm and 25.8 nm, respectively. This increase in size indicate the the formation of supramolecular assemblies between the cys-GQDs and the ZnPcs (**2a**, **2b**).

In FT-IR spectrum, the characteristic vibration corresponding to C≡N was observed at 2232 cm^{-1} for both phthalonitrile (**1a**, **1b**), the C—O—C vibration was observed at 1249 cm^{-1}, 1250 cm^{-1} for compound **1a** and **1b**, respectively. Aromatic C—H peak was seen at 3081 cm^{-1} for **1a** and between 3000–3100 cm^{-1} for **1b**. The C═C vibration was at 1589 cm^{-1}1, 1590 cm^{-1} for **1a** and **1b**, respevtively. The C—Br vibration was observed at 794 cm^{-1} for 1a and the C—Cl vibration was observed at 799 cm^{-1} for **1b**. The compounds **1a** and **1b** were cyclotetramerized using zinc acetate salt to produce zinc phthalocyanines derivatives. After conversion, the characteristic C≡N peaks disappeared on the FT-IR spectra of **2a** and **2b** due to the formation of phthalocyanine. The characteristic C—O—C vibration was observed at 1205 cm^{-1} for both phthalocyanines. Aromatic C—H peak was seen at 3281 cm^{-1}, 3252 cm^{-1}respectively for **2a** and **2b**. The other vibrations for C═C were at 1597 cm^{-1} for both **2a** and **2b**. The C—Br vibration for **2a** and C—Cl vibration for **2b** was observed at 744 cm^{-1}. ^{1}HNMR spectra of the synthesized compounds, **1a**: (500 MHz, δppm): Protons found as 7.75 (s, 1H, Ar—H), 7.73 (s, 1H, Ar—H), 7.54 (d, 2H, Ar-38H), 7.37 (d, 2H, Ar—H), 1.59 (s, 3H, —CH_3) and their integral values are in harmony. **1b**: Protons found as 7.75 (s, 1H, Ar—H), 7.73 (s, 1H, Ar—H), 7.57 (d, 2H, ArH), 7.08–7.06 (d, 2H, Ar—H), 1.58 (s, 3H, —CH_3) and their integral values are in harmony. **2a**: (500 MHz, δppm): Protons found as 7.86–7.49 (m, 24H, Ar—H), 1.59 (s, 12H, —CH_3) and their integral values are in harmony. **2b**: Protons found as 7.83–7.35 (m, 24H, Ar—H), 1.60 (s, 12H, —CH_3) and their integral values are in harmony. The hypothesized structures were supported by the mass spectra of all synthesized phthalocyanine complexes, with the parent ions at *m/z*: 310.787 $[M-2H]^+$ for **1a**, 270.883 $[M+2H]^+$ for **1b**, 1318.45 $[M]^+$ for **2a**, 1140.707 $[M]^+$ for **2b**. The characterization spectra of all the synthesized compounds are illustrated in the supplementary information Figs. S1–S12.

Fourier transform infrared (FT-IR) spectroscopy was further also used to characterize the cys-GQDs and the cys-GQDs–ZnPc conjugates. The FTIR spectrum of cys-GQDs shows the existence of the functional groupslocalized at the edges/surface of graphene quantum dots. The band at 1709 cm^{-1} for NGQD is attributed to C═ O vibration of the carboxyl group.The broad band arising in the range 3402–3196 cm^{-1} is due to the presence of functional groups like —OH and NH_2. The peaks at 1519, 1393 and 1232 and 1204 cm^{-1} can be attributed to N—H

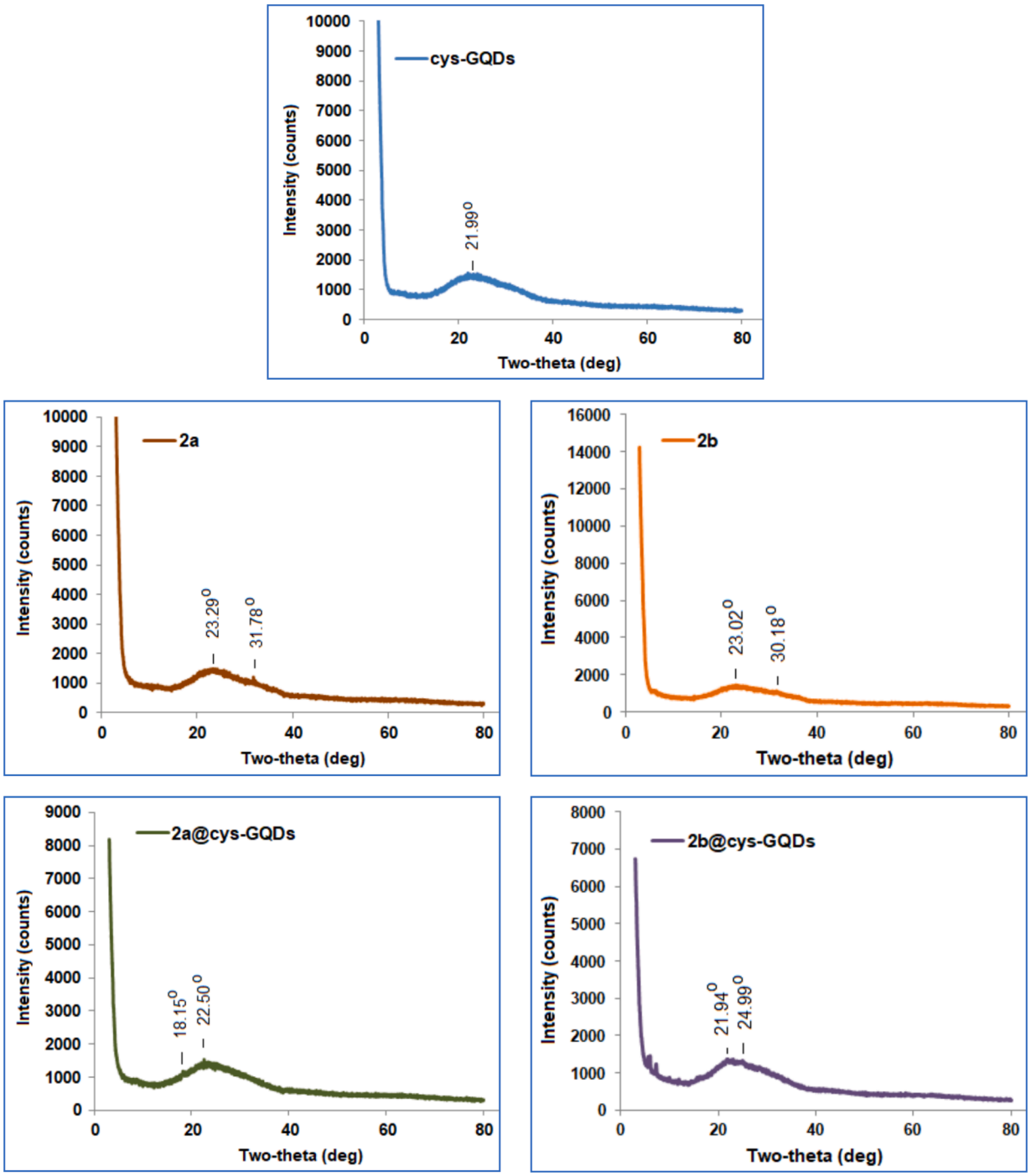


Fig. 5. X-ray diffraction patterns of cys-GQDs, **2a**, **2a**@cys-GQDs, **2b** and **2b**@cys-GQDs.

bending, C═C, C—N, C—O and C—S stretching vibrations. In addition, two bands at 2986 cm^{-1} and 2939 cm^{-1} are associated with the asymmetric and symmetric stretching of —CH_2 groups. Upon conjugation, C═ O vibration of the carboxyl group was seen at 1707 cm^{-1} for **2a**@cys-GQDs and 1712 cm^{-1} for **2b**@cys-GQDs. O—H vibrations revealed at 3266 cm^{-1} for **2a**@cys-GQDs and 3428 cm^{-1} for **2b**@cys-GQDs. The peaks arising from the C═C, C—N, C—O and C—S stretching vibrations were observed at 1598, 1392, 1240, 1205 cm^{-1} and 1561, 1311, 1245, 1207 cm^{-1}, for **2a**@cys-GQDs and **2b**@cys-GQDs, respectively. The peaks belonging to the ZnPcs (**2a** and **2b**) were observed at the FT-IR of the conjugates confirming the loading of the ZnPcs (**2a** and **2b**) onto the cys-GQDs, Fig. 4.

The X-ray powder diffraction (XRD) patterns of the prepared cys-GQDs, ZnPcs (**2a**, **2b**) before and after conjugation with cys-GQDs to form **2a**@cys-GQDs and **2b**@cys-GQDs are shown in Fig. 5. The XRD diffractogram of cys-GQDs shows a main broad band with a maximum at approximately 2Θ = 21.99° which is due to (002) Bragg's reflection of the carbon in the graphene layers [38]. The XRD patterns of the ZnPcs (**2a**, **2b**) alone are observed at 2Θ = 23.29° for **2a** and 2Θ = 23.02° for **2b** and are broad due to the amorphous nature of phthalocyanines [39]. The sharp peaks observed at 2Θ = 31.78° for **2a** and 2Θ = 30.18° for **2b** are indicative for crystalline structure of ZnPcs. **2a**@cys-GQDs and **2b**@cys-GQDs showed similar diffraction peaks as broad but shifted to 2Θ = 22.50° and 2Θ = 21.94°, respectively, as compared to Pcs alone. This is the indication of the presence of the interaction between cys-GQDs and ZnPcs (**2a**, **2b**).

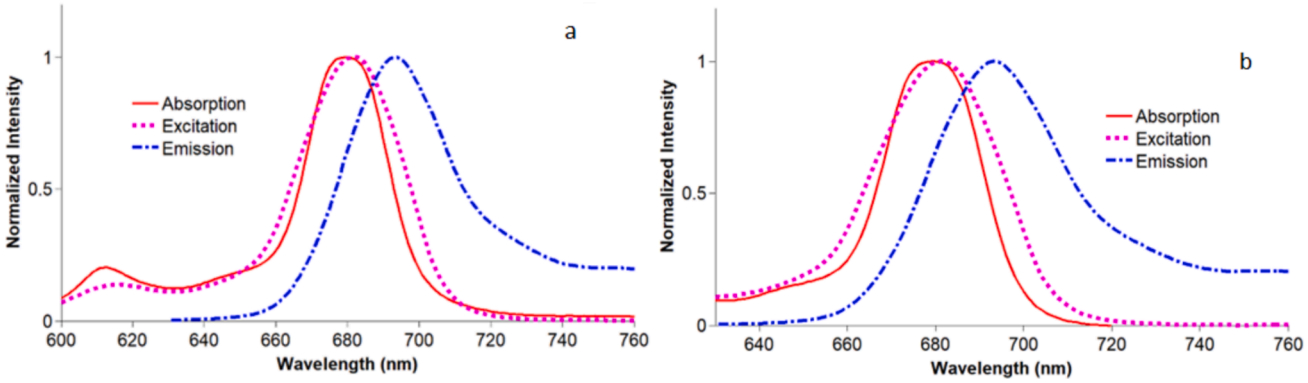


Fig. 6. Absorption (680 for both), excitation (681 for both) and emission (693 for both) spectra of (a) compound **2a**, (b) compound **2b** in DMSO.

Table 1
The quantum yields of the synthesized compounds.

Compound in DMSO	Φ_F	Φ_d (10^{-5})	$\Phi_{\Delta(PDT)}$	$\Phi_{\Delta(SPDT)}$
2a	0.20	5.0	0.63	0.94
2b	0.24	6.1	0.55	0.91
QD-2a	–	2.3	0.68	0.95
QD-2b	–	3.7	0.57	0.93
Unsubstituted ZnPc	0.20	–	0.67	–

3.2. *Fluorescence spectra and quantum yields (Φ_F)*

Fluorescence quantum yield (Φ_F) plays a critical role in anticancer therapies as it measures the sensitizer's ability to emit fluorescence, directly indicating its effectiveness in therapeutic applications. The Φ_F value is the ratio of emitted photons to absorbed photons. This parameter is crucial for evaluating the effectiveness of these complexes as sensitizers in photodynamic and/or sono-photodynamic therapy [40,41]. In this study, fluorescence assessments were conducted using solutions of synthesized phthalocyanine compounds in DMSO, with an absorbance level of around 0.5. Fig. 6 shows the absorption, fluorescence excitation and emission spectra of **2a** and **2b**. The absorption spectrum indicates the wavelengths of light absorbed by the compound. Meanwhile, the excitation spectrum identifies the wavelengths of light that cause the compound to become excited. The emission spectrum displays the wavelengths of light that are emitted by the compound following excitation.The fluorescence quantum efficiency of the compound **2a** is the same as the unsubstituted ZnPc we used as a standard, and it is $\Phi_F = 0.20$ [42] and **2b** was measured as $\Phi_F = 0.24$ (Table 1). Low fluorescence emission enhances intersystem crossing, a process where molecules transition between different energy states. This increased intersystem crossing allows molecules to move into higher-energy triplet states, resulting in higher levels of singlet oxygen formation, which is crucial for the effectiveness of photodynamic therapy.

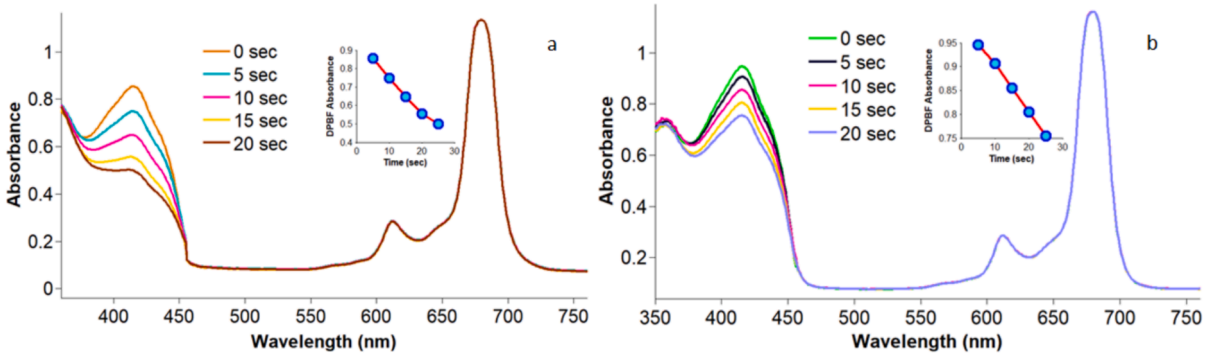


Fig. 7. The change in UV–Vis spectrum of the singlet oxygen quantum yield measurement of (a) compound **2a**, (b) compound **2b** by photochemical study.

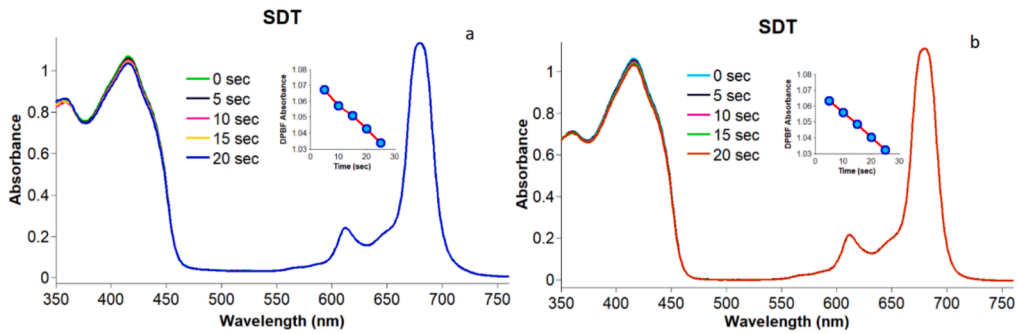


Fig. 8. The change in UV–Vis spectrum of the singlet oxygen quantum yield measurement of (a) compound **2a**, (b) compound **2b** by sonochemical study.

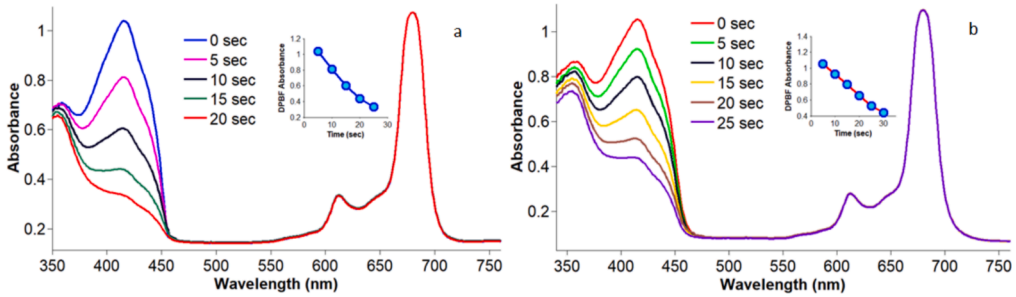


Fig. 9. The change in UV–Vis spectrum of the singlet oxygen quantum yield measurement of (a) compound **2a**, (b) compound **2b** by sono-photochemical study.

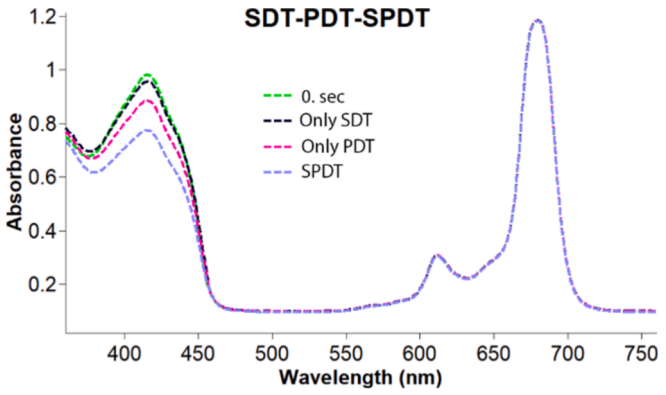


Fig. 10. The comparison of sonochemical, photochemical and sono-photochemical of compound **2b**.

3.3. Photochemical properties

3.3.1. Singlet oxygen quantum yields (Φ_Δ)

Singlet oxygen quantum yield is a measure of a molecule's ability to produce singlet oxygen. It is considered the most important factor in evaluating its potential as a sensitizer [43]. In this study, singlet oxygen quantum yields were measured by adding 1,3-diphenylisobenzofuran (DPBF) as a singlet oxygen quencher to the solutions of synthesized phthalocyanines. Standard ZnPc compounds were also prepared in DMSO as a comparison. In photochemical studies; UV–Vis spectra were obtained by exposing each sample to light of 7.05×10^{15} photon s^{-1} cm^{-2} intensity at each 5 s intervals for measurements, and recording the change in absorption of the DPBF compound at approximately 417 nm. Since the DPBF compound is sensitive to light and deteriorates during these measurements, all solutions were prepared in the dark. The singlet oxygen quantum yields of the synthesized compounds are given in Table 1. In the photochemical studies of the compound **2a**, the singlet oxygen quantum yield was calculated as 0.63, and the compound **2b** as 0.55. The Φ_Δ value of the ZnPc complex we used as a standard is 0.67 in DMSO [44]. Despite being lower than those of unsubstituted ZnPc in DMSO, the Φ_Δ values are still adequate for photodynamic therapy. In sonochemical studies; UV–Vis spectra were obtained by exposing each sample to ultrasound waves at each 5 s intervals for measurements, and recording the change in absorption of the DPBF compound at approximately 417 nm. Since there is no calculation method for sonochemical studies in the literature, only the DPBF reductions in the UV–Vis spectrum were checked and interpreted by comparing them with the photochemical method. The lower singlet oxygen yield observed in sonochemical studies compared to photochemical studies can be attributed to the fact that sound waves are generally less effective than light in generating singlet oxygen. Although sound waves can penetrate deeper into materials, their effectiveness in this context is limited. In sono-photochemical studies, each sample is initially exposed to ultrasound waves for 5 s, followed by exposure to light with an intensity of 7.05×10^{15} photon s^{-1} cm^{-2} for an additional 5 s. This process is repeated five times, during which the change in the absorption of the DPBF compound at approximately 417 nm is recorded, allowing for the monitoring of UV–Vis spectra. In sono-photochemical studies of compound **2a**, the singlet oxygen quantum efficiency was calculated as 0.94, and for compound **2b** as 0.91. Comparing the obtained results, it is seen that the singlet oxygen quantum yield obtained by sono-photochemical determination is significantly higher than that obtained by photochemical or sonochemical methods alone. Furthermore, the molecule containing Br exhibits a greater singlet oxygen quantum yield compared to the molecule containing Cl. This is because the molecular weight of Br element is higher than Cl element. This facilitates the transition between systems and causes more singlet oxygen to be formed [45]. UV–Vis spectra of singlet oxygen quantum yield measurements of synthesized compounds are given in Fig. 7–9. Sonochemical, photochemical and sono-photochemical comparison graph shown in Fig.10. It was observed that the singlet oxygen yield increased in the measurements taken after

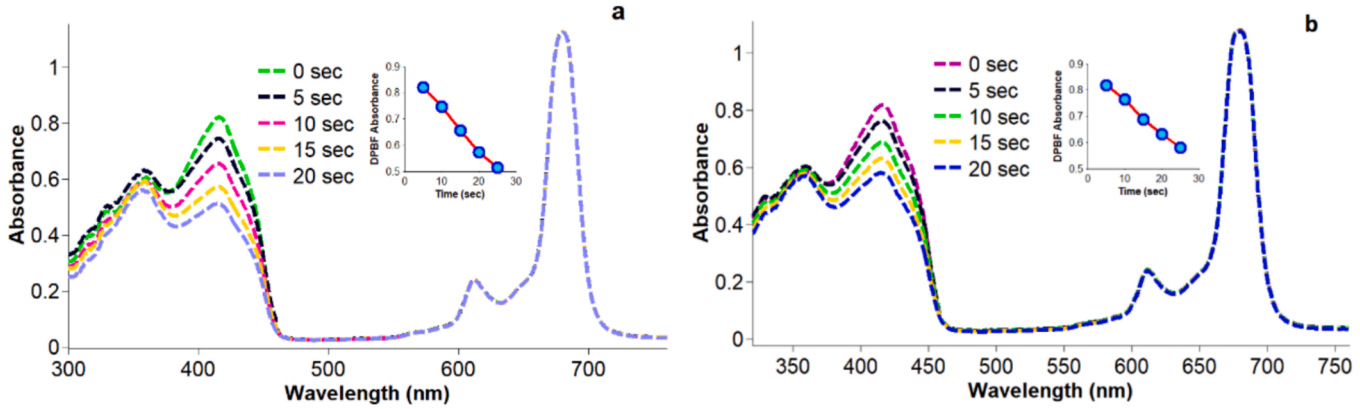


Fig. 11. The change in UV–Vis spectrum of the singlet oxygen quantum yield measurement of (a) **2a**@ cys-GQDs, (b) **2b**@ cys-GQDs by photochemical study.

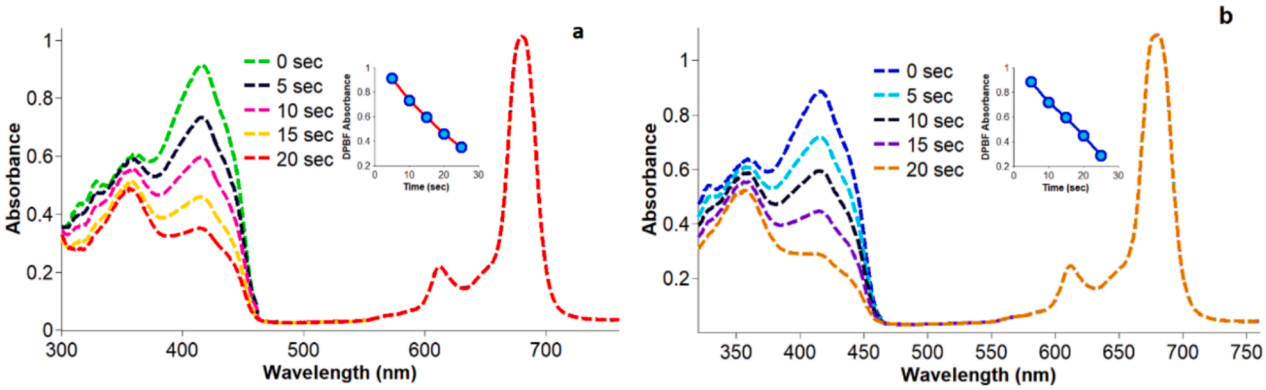


Fig. 12. The change in UV–Vis spectrum of the singlet oxygen quantum yield measurement of (a) **2a**@ cys-GQDs, (b) **2b**@ cys-GQDs by sono-photochemical study.

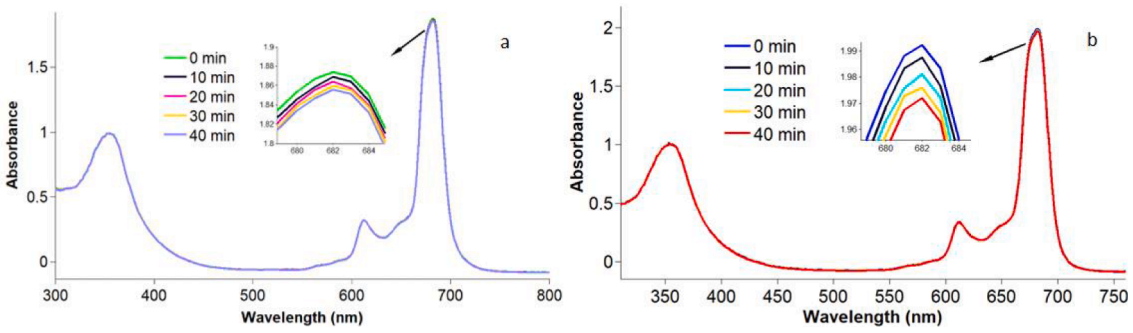


Fig. 13. The change in UV–Vis spectrum of photodegradationquantum efficiency measurement of (a) compound **2a**, (b) compound **2b**.

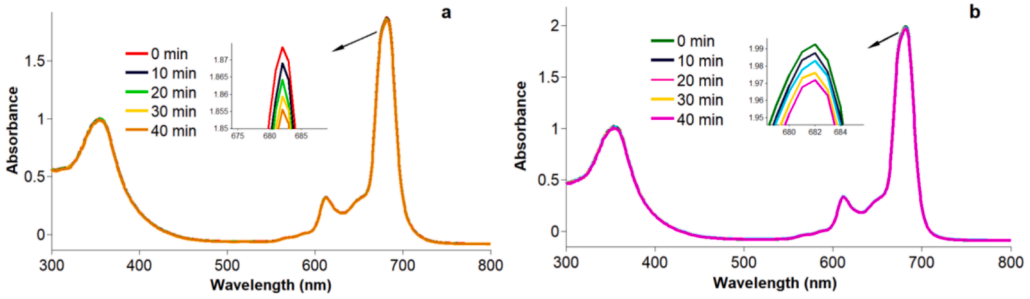


Fig. 14. The change in UV–Vis spectrum of photodegradationquantum efficiency measurement of (a) **2a**@ cys-GQDs, (b) **2b**@ cys-GQDs.

the combination of all synthesized phthalocyanines and the cysteine functionalized GQDs (cys-GQDs). In the photochemical studies of the compound **2a**@cys-GQDs, the singlet oxygen quantum yield was calculated as 0.68, and the compound **2b**@cys-GQDs as 0.57. In sono-photochemical studies of compound **2a**@cys-GQDs, the singlet oxygen quantum efficiency was calculated as 0.95, and for compound **2b**@cys-GQDsas 0.93. The singlet oxygen quantum yields of **2a**@cys-GQDs and **2b**@cys-GQDscompounds are given in Table 1. UV–Vis spectra of singlet oxygen quantum yield measurements of **2a**@cys-GQDs and **2b**@cys-GQDs are given in Fig. 11 and 12.

In all measurements taken in DMSO, it was observed that there was no significant difference in singlet oxygen yield. However, in cell culture studies conducted in media, it was observed that these types of molecules prepared were more effective by taking advantage of the drug carrier properties of quantum dots and their ability to increase solubility in aqueous media" was added into manuscript [46].

3.3.2. *Photodegradation quantum yields (Φ_d)*

In photochemical studies, the term photodegradation refers to the process where the photosensitizers used undergo chemical changes or degradation when exposed to light. Photosensitizers are compounds that target cells or tissues and are sensitive to light. However, when these compounds are exposed to light, they can undergo changes or break down in their structure. The photodegradation process can affect the effectiveness of photochemical studies and the long-term stability of photosensitizers. Therefore, the photodegradation properties of photosensitizers are an important evaluation criterion in PDT studies [47–49]. Photodegradation quantum yield was measured by first dissolving the synthesized compounds in DMSO. Subsequently, they were exposed to light with an intensity of 2.42×10^{16} s^{-1} cm^{-2} photon at 5-minute intervals. The change in absorption within the 600–800 nm range corresponding to the Q band was measured, resulting in the recording of UV–Vis spectra. The photodegradation quantum values were calculated as $\Phi_d = 5.0 \times 10^{-5}$ for the compound **2a** and as $\Phi_d = 6.1x10^{-5}$ for the compound **2b,** $\Phi_d = 2.3 \times 10^{-5}$ for the compound **2a**@ cys-GQDs and $\Phi_d = 3.7 \times 10^{-5}$ for the compound **2b**@ cys-GQDs. The quantum yields were given Table 1. It was observed that the cysteine functionalized GQDs (cys-GQDs) were more stable towards light irradiation. As

reported in the literature, stable complexes exhibit photodegradation capacities typically ranging between 10^{-6} and 10^{-3} [50,51]. This indicates that the synthesized complexes are resistant to light-induced decomposition, making them suitable for use in PDT and SPDT applications. The changes in the UV–Vis spectra of the photodegradation studies of the synthesized complexes are given in Figs. 13 and 14.

4. Conclusion

Substituent selection plays an important role in increasing the therapeutic effect of phthalocyanines synthesized for photosensitizer purposes. In this study, the effect of substituent groups was investigated by working with two different weights of atom (Br, Cl) for heavy atom effect, and conjugation with graphene quantum dots. In addition to the substituent effect, it was aimed to improve the singlet oxygen efficiency with 3 different methods (sonochemical, photochemical and sono-photochemical) applied. For this purpose, 2-Bromo-4-methylphenol zinc (II) phthalocyanine (**2a**) and 2-Chloro-4-methylphenol zinc (II) phthalocyanine (**2b**) were synthesized and characterized with the UV–Vis, FT-IR, ^{1}H NMR and MALDI-TOF mass spectrometry measurements. Both compounds are very soluble in organic solvents and do not show aggregation. Upon examining the yields of singlet oxygen, it was observed that compound **2a**, which contains Br, exhibits a higher quantum yield than compound **2b**, which contains Cl, across all irradiation methods. This enhancement is based on the presence of heavier atoms, which facilitate transitions between systems more effectively. When comparing the methods, the singlet oxygen generation potential of the sono-photochemical method was found to be higher than that of the photochemical and sonochemical methods alone. Since the quantum yields obtained in the photodegradation study are in between 10^{-3} and 10^{-6}, which are used as a measure in determining the stability of a substance in the literature, we can say that all synthesized compounds are stable to light.

In the second part of the study, Zn(II) phthalocyanine complexes (**2a**, **2b**) were successfully conjugated to cystein functionalized graphene quantum dots through π–π interaction and characterized. The sono-photochemical measurements were performed and compared with non-conjugated phthalocyanines. According to the results, the phthalocyanines conjugated with graphene quantum dots have higher singlet oxygen quantum yields for all irradiated methods. This is because quantum dots increase the formation of singlet oxygen. This could attributed to increased solubility in organic solvents.

In light of these results, we can say that the synthesized substances can be a good photosensitizer candidate to show therapeutic efficacy.

CRediT authorship contribution statement

Gökçe Gökçil: Writing – review & editing, Writing – original draft, Resources, Investigation, Formal analysis. **Göknur Yaşa Atmaca:** Writing – review & editing, Writing – original draft, Supervision, Investigation, Formal analysis. **Pınar Şen:** Writing – review & editing, Writing – original draft, Resources, Formal analysis. **Fikrettin Şahin:** Writing – review & editing, Supervision. **Ali Erdoğmuş:** Writing – review & editing, Supervision.

Declaration of competing interest

The authors declare that they have no known competing financial interests or personal relationships that could have appeared to influence the work reported in this paper.

Acknowledgments

This study was supported by Yildiz Technical University, Scientific Research Projects Coordination Unit (Project No.: FCD-2023-5812).

Appendix A. Supplementary material

Supplementary data to this article can be found online at https://doi.org/10.1016/j.jphotochem.2024.116108.

Data availability

No data was used for the research described in the article.

References

[1] G.Y. Atmaca, Polyhedron 193 (2021) 114894, https://doi.org/10.1016/j.poly.2020.114894.
[2] Y. Liu, P. Wang, Q. Liu, X. Wang, Ultrason. Sonochem. 31 (2016) 437–448, https://doi.org/10.1016/j.ultsonch.2016.01.038.
[3] D.O. Oluwole, F.A. Sarı, E. Prinsloo, E. Dube, A. Yuzer, T. Nyokong, M. Ince, Spectrochim. Acta Part A: Mol. Biomol. Spectrosc. 203 (2018) 236–243, https://doi.org/10.1016/j.saa.2018.05.090.
[4] B.D. Zheng, J. Ye, X.Q. Zhang, N. Zhang, M.T. Xiao, Coord. Chem. Rev. 447 (2021) 214155, https://doi.org/10.1016/j.ccr.2021.214155.
[5] N. Nomikou, K. Curtis, C. McEwan, B.M.G. O'Hagan, B. Callan, J.F. Callan, A. P. McHal, Acta Biomater. 49 (2017) 414–421, https://doi.org/10.1016/j.actbio.2016.11.031.
[6] Y. Zheng, J. Ye, Z. Li, H. Chen, Y. Gau, Acta Pharm. Sin. B 11 (8) (2021) 2197–2219, https://doi.org/10.1016/j.apsb.2020.12.016.
[7] G.Y. Atmaca, Inorg. Chim. Acta 515 (2021) 120052, https://doi.org/10.1016/j.ica.2020.120052.
[8] S.A.A. El-Kareem, G.H.A. Elsamie, A.S.A. Alkareem, Biochem.. Biophys. Res. Commun. 503 (2018) 1075–1086, https://doi.org/10.1016/j.bbrc.2018.06.119.
[9] M. Yüzeroğlu, G.K. Karaoğlan, G.G. Köse, A. Erdoğmuş, J. Mol. Struct. 1238 (2021) 130423, https://doi.org/10.1016/j.molstruc.2021.130423.
[10] H.J. Chen, X.B. Zhou, A.L. Wang, B.Y. Zheng, C.K. Yeh, J.D. Huang, Eur. J. Med. Chem. 145 (2018) 86–95, https://doi.org/10.1016/j.ejmech.2017.12.091.
[11] H. Chen, X. Zhou, Y. Gau, B. Zheng, F. Tang, J. Huang, Drug Discov. Today 19 (4) (2014) 502–509, https://doi.org/10.1016/j.drudis.2014.01.010.
[12] D. Costley, C.M. Ewan, C. Fowley, A.P. McHale, J. Atchison, N. Nomikou, J. F. Callan, Treat. Cancer Sonodyn. Ther.: Rev. 31 (2) (2015) 107–117, https://doi.org/10.3109/02656736.2014.992484.
[13] G.Y. Atmaca, C.C. Karanlık, A. Erdoğmuş, Dyes Pigm. 194 (2021) 109630, https://doi.org/10.1016/j.dyepig.2021.109630.
[14] Q. Li, Q. Liu, P. Wang, X. Feng, A. Wang, X. Wang, Ultrasonics 54 (4) (2014) 981–989, https://doi.org/10.1016/j.ultras.2013.11.009.
[15] Ö.D. Kutlu, F.A. Kılıçarslan, A. Erdoğmuş, Polyhedron 262 (2024) 117174, https://doi.org/10.1016/j.poly.2024.117174.
[16] G.Y. Atmaca, J. Mol. Struct. 1226 (2021) 129320, https://doi.org/10.1016/j.molstruc.2020.129320.
[17] G.Y. Atmaca, M. Aksel, B. Keskin, M.D. Bilgin, A. Erdoğmuş, Dyes Pigm. 184 (2021) 108760, https://doi.org/10.1016/j.dyepig.2020.108760.
[18] Y. Baygu, N. Kabay, B. Kabay, B. Yıldız, İ. Ömeroğlu, M. Durmuş, E.R. Karagür, H. Akça, Ç. Ergin, Y. Gök, J. Mol. Struct. (2022) 134010, https://doi.org/10.1016/j.molstruc.2022.134010.
[19] L. Hu, H. Han, Z. Xu, K. Song, F. Wang, J. Mol. Struct. 1291 (2023) 136007, https://doi.org/10.1016/j.molstruc.2023.136007.
[20] B. Koca, E. Hamuryudan, S. Catak, A. Erdogmus, A. Monari, V. Aviyente, J. Phys. Chem. C 123 (40) (2019) 24417–24425, https://doi.org/10.1021/acs.jpcc.9b07053.
[21] E. Güzel, B.S. Arslan, G.Y. Atmaca, M. Nebioğlu, A. Erdoğmuş, Chemistry Select 4 (2) (2019) 515–520, https://doi.org/10.1002/slct.201803255.
[22] A.A.H. Abdellatif, M.A. Younis, M. Alsharidah, O. Al Rugaie, H.M. Tawfeek, Int. J. Nanomed. 17 (2022) 1951–1970, https://doi.org/10.2147/IJN.S357980.
[23] Q. Xu, Q. Zhou, Z. Hua, Q. Xue, C. Zhang, X. Wang, D. Pan, M. Xiao, ACS Nano 7 (12) (2013) 10654–10661.
[24] S. Zhu, J. Zhang, C. Qiao, S. Tang, Y. Li, W. Yuan, B. Li, L. Tian, F. Liu, R. Hu, H. Gao, H. Wei, H. Zhang, H. Sun, B. Yang, Chem. Commun. 24 (2011) 6858, https://doi.org/10.1039/C1CC11122A.
[25] S. Benitez-Martinez, M. Valcarcel, Sensor. Actuator. B Chem. 197 (2014) 350–357, https://doi.org/10.1016/j.snb.2014.03.008.
[26] Z. Wang, J. Xia, C. Zhou, B. Via, Y. Xia, F. Zhang, Y. Li, L. Xia, J. Tang, Colloids Surf. B: Biointerfaces 112 (2013) 192–196, https://doi.org/10.1016/j.colsurfb.2013.07.025.
[27] M. Managa, O.J. Achadu, T. Nyokong, Dyes Pigm. 148 (2018) 405–416, https://doi.org/10.1016/j.dyepig.2017.09.031.
[28] M.J. Sweetman, S.M. Hickey, D.A. Brooks, J.D. Hayball, S.E. Plush, Adv. Funct. Mater. 29 (14) (2019) 1808740, https://doi.org/10.1002/adfm.201808740.
[29] J. Ge, M. Lan, B. Zhou, W. Liu, L. Guo, H. Wang, Q. Jia, G. Niu, X. Huang, H. Zhou, X. Meng, P. Wang, C.S. Lee, W. Zhang, X. Han, Nat. Commun. 5 (2014) 4596, https://doi.org/10.1038/ncomms5596.
[30] N. Sahiner, S.S. Suner, M. Sahiner, C. Silan, J. Fluoresc. 29 (2019) 1191–1200, https://doi.org/10.1007/s10895-019-02431-y.
[31] S.A. Majeed, N. Nwaji, J. Mack, T. Nyokong, S. Makhseed, J. Lumin. 213 (2019) 88–97, https://doi.org/10.1016/j.jlumin.2019.04.034.
[32] M. Kandaz, M.N.U. Yaraşir, A. Koca, Ö. Bekaroğlu, Polyhedron 21 (3) (2002) 255–263, https://doi.org/10.1016/S0277-5387(01)00982-2.

[33] M. Özer, A. Altındal, A.R. Özkaya, M. Bulut, Ö. Bekaroğlu, Polyhedron 25 (18) (2006) 3593–3602, https://doi.org/10.1016/j.poly.2006.07.011.
[34] Y.W. Zeng, D.K. Ma, W. Wang, J.J. Chen, L. Zhou, Y.Z. Zheng, K. Yu, S.M. Huang, Appl. Surf. Sci. 342 (2015) 136–143, https://doi.org/10.1016/j.apsusc.2015.03.029.
[35] S. Shi, H. Liu, T. Chen, C. Chen, B. Ko, Front. Mater. 10 (2023) 1–8, https://doi.org/10.3389/fmats.2023.1180745.
[36] Y.I. Openda, P. Sen, M. Managa, T. Nyokong, Photodiagn. Photodyn. Ther. 29 (2020) 101607, https://doi.org/10.1016/j.pdpdt.2019.101607.
[37] S. Kim, S.W. Hwang, M.K. Kim, D.Y. Shin, D.H. Shin, C.O. Kim, S.B. Yang, J. H. Park, E. Hwang, S.H. Choi, G. Ko, S. Sim, C. Sone, H.J. Choi, S. Bae, B.H. Hong, ACS Nano 6 (9) (2012) 8203–8208, https://doi.org/10.1021/nn302878r.
[38] O.J. Achadu, T. Nyokong, New J. Chem. 41 (4) (2017) 1447–1458, https://doi.org/10.1039/C6NJ03285K.
[39] O.J. Achadu, I. Uddin, T. Nyokong, J. Photochem. Photobiol. A Chem. 317 (2016) 12–25, https://doi.org/10.1016/j.jphotochem.2015.11.006.
[40] G.Y. Atmaca, K. Celep, A. Erdoğmuş, J. Organometall. Chem. 1004 (2024) 122952, https://doi.org/10.1016/j.jorganchem.2023.122952.
[41] H. Messaoudi, G.Y. Atmaca, A. Erdoğmuş, J. Mol. Struct. 1312 (2024) 138394, https://doi.org/10.1016/j.molstruc.2024.138394.
[42] E. Kırbaç, G.Y. Atmaca, A. Erdoğmuş, J. Organomet. Chem. 752 (2014) 115–122, https://doi.org/10.1016/j.jorganchem.2013.12.005.
[43] Ö.D. Kutlu, A. Erdoğmuş, P. Şen, S.Z. Yıldız, J. Mol. Struct. 1284 (2023) 135375, https://doi.org/10.1016/j.molstruc.2023.135375.
[44] M. Durmuş, T. Nyokong, Spectrochim. Acta Part A: Mol. Biomol. Spectrosc. 69 (4) (2008) 1170–1177, https://doi.org/10.1016/j.saa.2007.06.029.
[45] J. Ribes, Y. Bourdeau, E. Rascol, I. Bestel, E. Badarua, Bioorg. Med. Chem. 81 (2023) 117210, https://doi.org/10.1016/j.bmc.2023.117210.
[46] P. Sen, T. Nyokong, Photodiagn. Photodyn. Ther. 34 (2021) 102300, https://doi.org/10.1016/j.pdpdt.2021.102300.
[47] M. Göksel, Bioorg. Med. Chem. 24 (18) (2016) 4152–4164, https://doi.org/10.1016/j.bmc.2016.07.003.
[48] K. Celep, G.Y. Atmaca, A. Erdoğmuş, J. Mol. Struct. 1299 (2024) 137021, https://doi.org/10.1016/j.molstruc.2023.137021.
[49] A. Erdoğmuş, M. Arıcı, J. Fluor. Chem. 166 (2014) 127–133, https://doi.org/10.1016/j.jfluchem.2014.08.005.
[50] B. Çoşut, S. Yeşilot, M. Durmuş, A. Kılıç, V. Ahsen, Polyhedron 29 (2) (2010) 675–682, https://doi.org/10.1016/j.poly.2009.09.035.
[51] Ş. Özçelik, G.K. Karaoğlan, G. Gümrükçü, A. Erdoğmuş,, A. Gül, J. Organomet. Chem. 769 (2014) 17–23, https://doi.org/10.1016/j.jorganchem.2014.06.024.